

Scaling sediment flux across landscapes

J. P. M. SYVITSKI & A. J. KETTNER

CSDMS Integration Facility, INSTAAR, University of Colorado — Boulder, Boulder, Colorado 80309-0545, USA
james.syvitski@colorado.edu

Abstract The BQART model is applied for the first time to the world's continents, to estimate the delivery of suspended sediment before (at 20 167 Mt/year) and after the interference by humans (presently at 12 838 Mt/year). Basin area is found to be the great integrator of relief, lithology, runoff, and humans. BQART is also used in a recursive manner to conceptually show the conveyance loss of suspended sediment along the pathway of rivers. Application of the Bagnold bed-material load equation to Space Shuttle Radar altimetry of river thalwegs is used to show the loss of sediment along the world's flood plains and other intra-continental sinks.

Key words coastal; modelling; global; sediment; flood plains; deltas

INTRODUCTION

Herein we discuss the principal factors that control the flux of fluvial sediment to the world's coastal ocean. We perform a global analysis of the sediment flux to the ocean based on an application of the BQART model, supported by state-of-the-art GIS grids of the controlling factors. The BQART model (Syvitski & Milliman, 2007) accounts for: (1) geomorphic and tectonic influences through the parameters basin area and basin relief; (2) geographical influences through basin temperature, water discharge, and glacier extent; (3) geological controls through basin-integrated lithology; and (4) human activities that may accelerate or mitigate soil erosion and/or trap sediment in reservoirs. BQART inherently incorporates the scaling of sediment production (chemical, mechanical and human erosion), sediment storage (lakes, reservoirs, flood plains) and flood-wave dynamics. Basin area appears as the overarching integrator, whether assessing flood dynamics, lithologic variability, or the competing influences of humans. When applied to a database of 488 rivers, the BQART model shows no ensemble over- or under-prediction, offering a bias of just 3% across six orders of magnitude in observational values, and accounts for 96% of the between-river variation on the long-term (± 30 years) sediment load or yield of these rivers (Syvitski & Milliman, 2007). Syvitski *et al.* (2005) conducted a similar analysis as shown below, but used the more limited QRT or ART models (Syvitski *et al.*, 2003) that did not fully parameterize the human factors, and did not include the influence of basin lithology and glacier erosion within its formulation.

BQART model summary

Syvitski & Morehead (1999) employed dimensional analysis to the problem of predicting a river basin's long-term sediment load Q_s (M/T), concentrating on the parameters relief R (L), drainage area A (L^2), fluid density ρ (M/L 3), and gravity g (L/T 2). Two dimensionless variables were shown to reflect gravity-driven sediment yield (left side of equation (1)), and a basin's potential energy (right side of equation (1)):

$$\frac{Q_s}{\rho g^{1/2} A^{5/4}} = \alpha \left(\frac{R}{A^{1/2}} \right)^n \quad (1)$$

where α and n are the empirical constants relating the dimensionless variables. Using the globally-averaged value of $n = 1$ (see Syvitski *et al.*, 2003), and the global relationship between discharge, Q , in m 3 /s, and drainage area, A , in km 2 ($Q = 0.075 A^{0.8}$), then Syvitski and Milliman showed that:

$$Q_s = w B Q^{0.31} A^{0.5} R \cdot T \text{ for } T \geq 2^\circ\text{C} \quad (2a)$$

$$Q_s = 2wB Q^{0.31} A^{0.5} R \quad \text{for } T < 2^\circ\text{C} \quad (2b)$$

where $w = 0.02$ for units of kg/s, or $w = 0.0006$ for units of MT/year, Q is in km³/year, A is in km², R is in km, and T is in °C. The B term accounts for important geological and human basin-wide factors missing from the ART or QRT models, and expands as:

$$B = IL(1 - T_E)E_h \quad (3)$$

I is the glacier erosion factor defined as $I = (1 + 0.09A_g)$, where A_g is the area of the drainage basin as a percent of the total drainage area. T_E is the trapping efficiency of lakes and man-made reservoirs, such that $(1 - T_E) \leq 1$.

The basin-averaged lithology factor (L) is defined as: $L = 0.5$ for basins comprised principally of hard, acid plutonic and/or high-grade metamorphic rocks, $L = 0.75$ for basins of mixed, mostly hard lithology, sometimes including shield material, $L = 1.0$ for basins of volcanic, mostly basaltic rocks, or carbonate outcrops, or mixture of hard and soft lithology, $L = 1.5$ for basins with a predominance of softer lithologies, but a significant area of harder lithologies. $L = 2.0$ for fluvial systems draining a significant proportion of sedimentary rocks, unconsolidated sedimentary cover, or alluvial deposits, and $L = 3$ for basins with an abundance of exceptionally weak material (crushed rock, loess deposits).

E_h is the human-influenced soil erosion factor, which may provide either a positive or negative influence on a river's sediment flux, and is based on population density and GNP per capita: $E_h = 0.3$ for basins with a high density population PD > 200 km², and a GNP/capita >\$15k/year. $E_h = 1$ for basins with a low human footprint (PD < 50 km²) or those containing a mixture of the competing influences of soil erosion and conservation. $E_h = 2.0$ for basins where the population is high (PD > 200 km²), but GNP/capita is low (<\$2.5k/year), and where basins have not received the resources to engineer solutions to problems of soil erosion.

Finally, BQART may be rewritten in terms of catchment yield Y_s for suspended load:

$$Y_s = wB Q^{0.31} A^{-0.5} R T \quad (4)$$

BASIN AREA AS THE GREAT INTEGRATOR

Basin area is the great integrator of competing forces that impact a catchment's sediment yield or load. The fractal nature of the Earth's surface means there are few giant river basins (Amazon, Congo), but many smaller basins. Larger basins inevitably have headwaters in a continent's highest mountain peaks, thus reflecting the scale of a continents tectonic history. Some small coastal rivers also drain high (coastal) mountains, but others drain lowlands. Large river basins also have significant lower elevation areas. The elevated sediment delivery from glacierized alpine environment is thus mitigated by the increased sediment storage capacity of their flood plains (e.g. Ganges). By their very size, large basins contain a range of regional lithologies, and thereby integrate delivery from easily erodible surfaces to more resistant rocks. Smaller basins, by contrast, are likely to be influenced by a narrower range in weathering and lithology.

The Earth's range in catchment area also leads to a partial independence between basin area and discharge. Giant basins, by their very size, incorporate both wet and dry regions, limiting their runoff values to less than 1 m/year. In contrast, smaller basins easily fit within a single climate zone and thus range from high (>2 m/year) to very low (<0.05 m/year) hydrological runoff values.

On the dynamic side, large rivers are more capable of dampening their flood waves through friction (wave height decreases with distance downstream), than smaller rivers. In addition, small (lower Strahler order) basins will often receive the impact of a storm front across its catchment at roughly the same time, whereas in higher order rivers the storm front can take days to cross the catchment. Flash flood activity is thus common in smaller catchments; discharge near the mouths of larger basins is often not much different from one day to the next.

Human activity, such as from deforestation, can more easily influence the magnitude of sediment delivery from a smaller basin (e.g. Eel River, USA), than from within a larger basin (e.g.

Amazon). An exception is through the impact of reservoirs that can just as easily separate a coastal region from its upland sediment supply in a large river (e.g. Colorado, Nile, Indus) than in a smaller river (e.g. Ebro).

GLOBAL APPLICATION OF BQART

To complete a global analysis of the sediment flux delivered to the world's coastal ocean we obtained geo-referenced data layers for each of the BQART terms (equations (2) and (3)), at a minimum resolution of 30 minutes (latitude \times longitude – approx. 60 000 grid cells). We next determined the integrated basin-wide parameter values for each of the 4464 river basins defined in the University of New Hampshire (UNH) Simulated Topological Network (STN-30p) for potential river flow paths (Syvitski *et al.*, 2005). These basins do not include the drainage basins covered by the ice sheets of Antarctica, Greenland and portions of the Canadian Archipelago, or those that do not have a positive discharge to the coastal ocean or sea (see Syvitski *et al.*, 2005 for details). Our data layers include the following:

- population density from 2000 (based on UNESCO data; <http://wwdrii.sr.unh.edu/download.html>);
- Gross National Income per capita (GNI) from 2005, formerly GNP (World Bank; <http://www.worldbank.org/>);
- lithology using a re-integration of the Dürr *et al.* (2005) digital lithology map onto STN-30p drainage basins (see Fig. 1);
- basin surface temperatures calculated from NCEP/NCAR Reanalysis data from the NOAA-CIRES Climate Diagnostic Center, averaged across 30-years (see Syvitski *et al.*, 2003a);
- relief obtained from the GTOPO-30 global digital elevation model established in 1996 (<http://edc.usgs.gov/products/elevation/gtopo30/gtopo30.html>);
- catchment areas using STN-30p have a 7.5% absolute error, and a 2% bias;
- ice cover from the National Snow and Ice Data Center (Armstrong, *et al.*, 2005);
- composite discharge field comes from monthly values (1970–1999) derived from the Global Runoff Data Centre (GRDC) covering 72% of the world's actively discharging landmass, merged with simulations based on modern climatology using the UNH Water Balance and Transport Model (WBM/WTM) to provide discharge values where observations are not available (see Syvitski *et al.*, 2005 for details);
- reservoir trapping embedded into the UNH WBM/WTM (Vörösmarty *et al.*, 2003; Syvitski *et al.*, 2005).

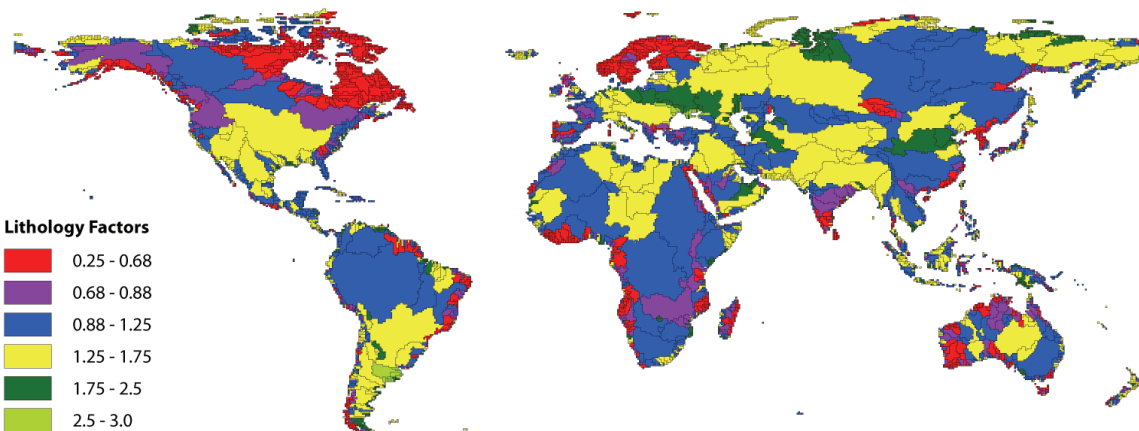


Fig. 1 Basin integrated lithology.

To arrive at the pre-human flux of sediment, we use the modern climatology (basin-averaged temperature and discharge), and we set E_h in equation (3) equal to 1, and assumed there were no artificial reservoirs. BQART then predicts a pre-human suspended sediment flux to the coastal ocean at 20 617 Mt/year (Table 1, Fig. 2). This value is larger than the initial estimate from Syvitski *et al.* (2005), who used a similar approach but applied the less sophisticated (ART) model that did not take into account sediment production from glaciers, or variable catchment lithology.

Table 1 Continental values of water discharge (Q) using combined GRDC observations and UNH WBM/WTM model simulations (Syvitski *et al.*, 2005); and both continental values of suspended sediment load (Q_s), circa late 20th century, using Syvitski & Milliman (2007) observations combined with BQART simulations, and pre-human Q_s load values using the BQART model (see text for details).

Continent	Q (km ³ /year)	Q_s with Humans (Mt/year)	Q_s pre-Humans (Mt/year)
Africa	3 797	1 201	2 438
Asia	9 806	4 293	6 977
Australasia	608	225	300
Europe	2 680	445	766
Indonesia	4 251	2 575	2 421
North America	5 819	1 357	2 130
Oceans	20	4	3
South America	11 529	2 738	5 582
Global	38 510	12 838	20 617

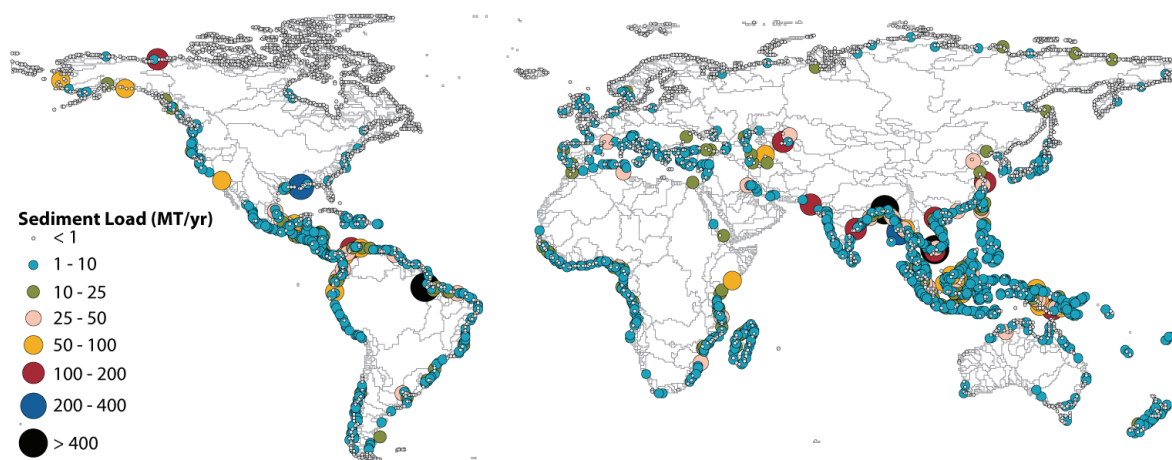


Fig. 2 BQART simulated suspended sediment load before the major imprint of humans.

The pre-Human flux (Table 2) was adjusted for the world's two largest rivers, the Amazon and the Congo, by adjusting their values to modern values — it is recognized that BQART over-predicts the sediment delivery on giant tropical rivers. There are competing hypothesis for this over-prediction by BQART. Firstly, the impact of a few high mountains may be over-emphasized, given the gigantic size of their catchments (e.g. Congo). Secondly, giant rivers often have significant intra-montane basins and foreland basin fans and flood plains that trap much of the seaward transiting sediment (e.g. Amazon). Thirdly, equatorial jungles may give up much less sediment on exceedingly flat flood plains, compared with more temperate basins. Testing these competing hypotheses is an active field of research.

Human-influenced sediment loads were based on observed loads (160 rivers with reliable observations between 1960 and 1990) merged with BQART estimates based on modern climatology, and human landscape use. The method predicts that 12 838 Mt/year are delivered to the coastal ocean as of the late 20th century. This value is within 8% of the QRT estimates from

Syvitski *et al.* (2005), the difference largely related to the newer values of observed sediment loads ingested into the composite approach (Fig. 3). For example the Yellow River had, during the period 1900 to 1960, sediment loads exceeding 1000 MT/year. The Yellow River load has steadily decreased to ≈ 100 Mt/year by the year 2000, largely related to interception of the load by upstream dams, and reduction in the water discharge to the delta (Wang *et al.*, 2007).

The difference between the updated human-influenced sediment loads (Fig. 3) and the new estimates of sediment delivery for the period before human disturbance (Fig. 2), suggests that ever more sediment is being trapped within reservoirs.

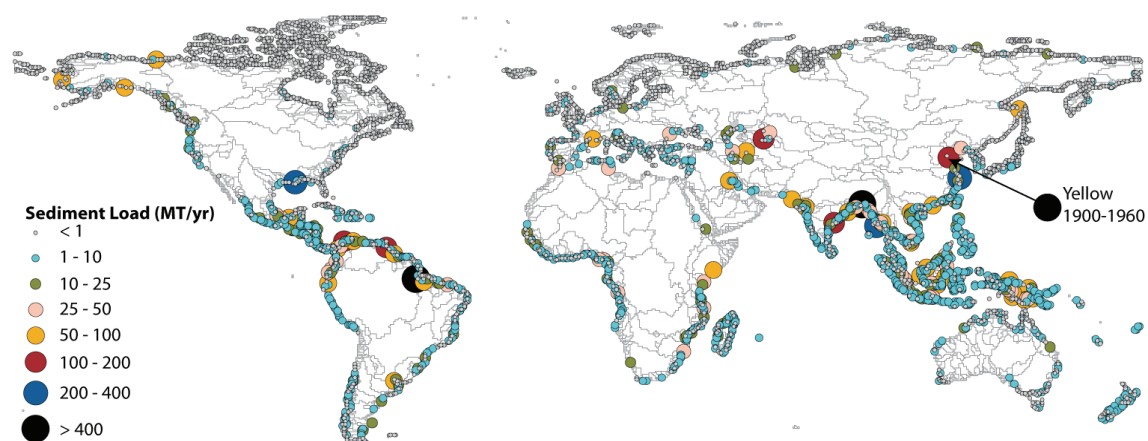


Fig. 3 BQART simulated suspended sediment load after the imprint of humans, c. 1990. Note that the size of the sediment loads is a moving target for many of the populated river basins. For example during 1900–1960, the sediment load of the Yellow River exceeded 1000 MT/year.

DELIVERY OF SEDIMENT WITHIN RIVER BASINS

BQART through equation (4) shows that sediment yield decreases as the size of the basin increases (Table 2), in agreement with observations. The decrease in yield relates to two factors: (1) local sediment yield from lower elevations is smaller than for the highland regions; and (2) sediment is sequestered along the transport path within, for example, intra-montane basins, foreland basin fans and flood plains. To demonstrate the potential sequestration of sediment, we apply BQART to an ideal temperate basin that sees runoff decreasing to the coast, yet discharge increasing to the coast (Table 2). The greatest elevation change (2.55 km) is located in the upper basin, with a 50 000 km² catchment area; the total basin area is set to 400 000 km² with a basin relief of 3.55 km (Table 2). BQART predicts for the upper basin a sediment load of 32.1 Mt/year, a value that increases as the stream progresses to the coast where the load reaches 158.8 Mt/year (Table 2). BQART also predicts that the sediment yield decreases from 643 MT/km² year in the upper basin, to 397 MT/km² year for the entire basin (Table 2). If the sediment yield were constant within the entire basin (e.g. set at the upper catchment value of 643 MT/km² year), then BQART predicts sediment load would increase from 32 to 257 Mt/year (Table 2). Differencing the two estimates of sediment load provides for a conveyance loss of 38.2% across the entire basin. This is the maximum theoretical value of sequestration of suspended sediment within this ideal basin, as yield would likely not be constant across the entire basin.

Rivers also transport a bed-material load, which may be calculated using a modified Bagnold (1966) equation:

$$Q_b = \frac{\rho_s}{\rho_s - \rho} \frac{\rho g Q^\beta S e_b}{\tan \phi} \quad \text{when } u \geq u_{cr} \quad (5)$$

where ρ_s and ρ is the density of sediment and water (kg/m³) respectively, g is the acceleration due to gravity (m/s²), S is the river thalweg (m/m), e_b is the bed-load efficiency (dimensionless), β is a

Table 2 Application of the BQART sediment load model to an ideal basin that sees runoff decreasing to the coast, and discharge increasing to the coast. The greatest elevation change (2.55 km) is in the upper basin with a 50 000 km² catchment area; the total basin area is 400 000 km² with a total basin relief of 3.55 km. See text for details.

Runoff (m/year)	Area (km ²)	Relief (km)	Q (km ³ /year)	BQART (Mt/year)	QBART yield (t/km ² year)	Yield est load (Mt/year)	Conveyance loss (%)
2.50	50 000	2.55	125	32	643	32	0
1.50	100 000	2.70	150	51	509	64	20.8
1.00	200 000	3.00	200	88	437	129	31.9
0.75	300 000	3.30	225	122	407	193	36.6
0.65	400 000	3.55	260	159	397	257	38.2

Table 3 Some characteristics of rivers in terms of catchment area (A), maximum relief (R), mean discharge (Q), mean suspended sediment load (Q_s), length (L) of main channel, and to 10 m and 100 m elevation above sea level along thalweg, bed load as calculated at 100 m above sea level and at 10 m above sea level, bed load lost between 10 m and 100 m above sea level, and the loss rate per kilometre of river thalweg.

River	A (km ²)	R (m)	Q (m ³ /s)	Q_s (kg/s)	L (km)	L to 100 m (km)	L to 10 m (km)	Q_b @ 100 m (kg/s)	Q_b @ 10 m (kg/s)	Q_b lost (%)	Q_b loss per km (kg/km)
Chao Phraya (Thai)	160 000	1 920	963	349	1 200	730	218	29	11	63	0.08
Fly (PNG)	64 400	3 990	2 510	2 219	1 130	901	577	70	11	85	0.10
Godavari (India)	287 000	1 650	2 650	5 387	1 450	513	95	137	69	50	0.72
Indus (Pak)	964 000	7 830	3 171	12 683	3 180	1 188	220	70	36	49	0.15
Irrawaddy (Burma)	430 000	5 881	13 558	8 239	2 150	1 078	337	338	99	71	0.71
Mekong (Viet)	811 000	6 100	14 770	5 070	4 425	1 008	566	783	64	92	1.27
Niger (Nig)	1 240 019	2 130	6 130	1 268	4 170	1 023	242	182	63	66	0.49
Po (Ita)	70 000	4 800	1 904	545	652	467	141	70	33	53	0.26
Rhone (Fr)	90 000	4 810	1 700	1 982	820	215	67	264	63	76	3.01
Euphrates (Iraq)	1 050 000	2 960	1 500	1 680	2 815	1 157	511	48	7	85	0.08
Vistula (Pol)	200 000	2 500	1 050	79	1 091	547	86	42	30	28	0.14
Yangtze (PRC)	1 958 000	6 800	28 278	15 210	4 670	1 771	840	642	83	87	0.67

bed-load rating term (dimensionless and set to 1 for this study), ϕ is the limiting angle of repose of sediment grains lying on the river bed, u is the stream velocity, and u_{cr} is the critical velocity below which no bed-load transport occurs.

Syvitski & Saito (2007) calculated the bed load as a percent of the total sediment load delivered to 51 global deltas; the values averaged 6.6%, with a range of 0.7% (Mississippi) to 30% (Kolyma). Table 3 provides a more advanced estimate of the bed load of 12 rivers, calculated across: (1) the distance between the river locations at 10 m and 100 m elevation above sea level, and (2) the distance between the coast (0 m) and the river location 10 m elevation above sea level. The data was derived using Space Shuttle Radar altimetry that has a 1-m vertical resolution. RiverTools ® was applied to determine the flow length of the major river channel (Fig. 4, Table 3). In all cases, bed load is much smaller than the suspended load. Between 49% and 92% of the bed load that passed by the 100 m elevation location is deposited before the 10 m elevation location is reached (Table 3). The rate loss for these rivers varies between 0.08 kg/km s for the Chao Phraya River and 3 kg/km s for the Rhone.

As a thought experiment, we create a small, high mountain basin, to demonstrate these concepts (Fig. 5(a)). Discharge increases down the length of the river (Fig. 5(b)). Using both Bagnold's equation to predict the bed-material load and BQART to predict the wash (suspended) load, Fig. 5(c) shows: (1) the suspended load carried down the main channel; (2) the bed load carried by the main channel; (3) bed load contributed by smaller tributary channels; and (4) the total load along the central channel. Bed load is the largest component for much of the river course

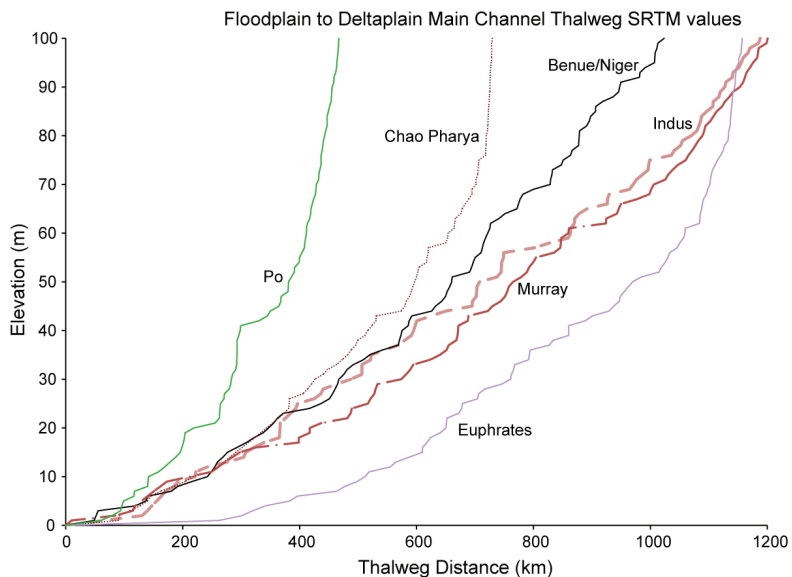


Fig. 4 Thalweg of river profiles sensed from the Space Shuttle using radar altimetry (SRTM).

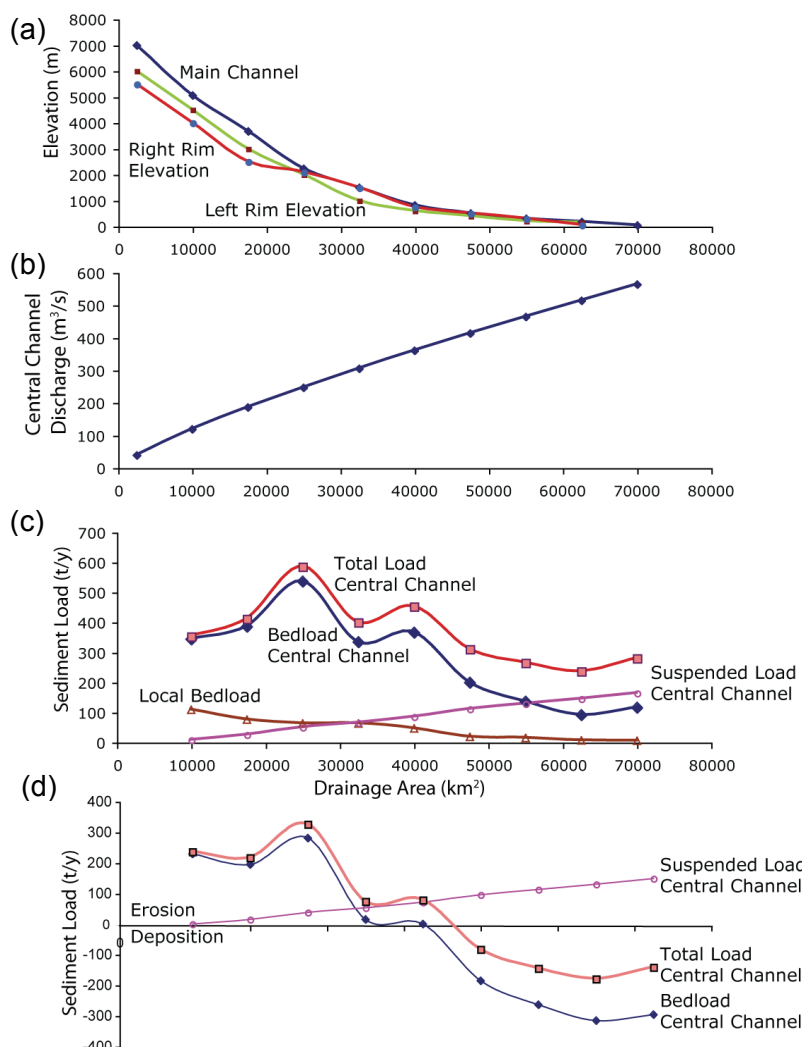


Fig. 5 Idealised small mountainous river basin: (a) Elevation-area relationships; (b) Discharge-area relationship. (c) Suspended load, bed load and total load carried by the main channel, and bed load contributions by tributary channels. (d) Zones of erosion and deposition within this ideal basin.

off of the highland, but suspended load becomes the larger component nearer the coast. Applying a recursive technique, it is seen that the river operates in an erosive form for about half of the river length, but eventually enters into a depositional mode.

Figure 4 displays wavy perturbations to the otherwise log-linear along-channel profiles crossing the flood plains of the major rivers. These are interpreted as sediment waves, from the crevasse splays and fans formed during major floods of the rivers and seen on SRTM imagery. The waves reflect the conveyance loss of the sediment loads delivered to the coast.

SUMMARY

While the experiments above remain primitive, they suggest a growing understanding on sediment production and transport within basins and delivery to the coastal ocean. This first global application of the BQART model provides further evidence on the growing human influence on sediment delivery. BQART incorporates many of the basin scaling relationships between basin properties, including area, relief, temperature, runoff, lithology, and ice cover. Combined with bed-material load equations (a modified-Bagnold used above), then BQART is shown to add value to our understanding of conveyance loss of sediment in intra-montane basins, fans, flood plains and deltas.

REFERENCES

- Armstrong, R., Raup, B., Khalsa, S. J. S., Barry, R., Kargel, J., Helm, C. & Kieffer, H. (2005) GLIMS glacier database. National Snow and Ice Data Center, Boulder, Colorado, USA (digital media).
- Dürr, H. H., Meybeck, M. & Dürr, S. H. (2005) Lithologic composition of the Earth's continental surfaces derived from a new digital map emphasizing riverine material transfer. *Global Biogeochem. Cycles* **19**, GB4S10, doi:10.1029/2005GB002515.
- Syvitski, J. P. & Morehead, M. D. (1999) Estimating river-sediment discharge to the ocean: application to the Eel Margin, northern California. *Marine Geology* **154**, 13–28.
- Syvitski, J. P. M. & Milliman, J. D. (2007) Geology, geography and humans battle for dominance over the delivery of sediment to the coastal ocean. *J. Geology* **115**, 1–19.
- Syvitski, J. P. M., Peckham, S. D., Hilberman, R. D. & Mulder, T. (2003) Predicting the terrestrial flux of sediment to the global ocean: a planetary perspective. *Sedimentary Geology* **162**, 5–24. Erratum *Sedimentary Geology* **164**, 345.
- Syvitski, J. P. M. & Saito, Y. (2007) Morphodynamics of deltas under the influence of humans. *Global Planetary Change* **57**, 261–282.
- Syvitski, J. P. M., Vörösmarty, C., Kettner, A. J. & Green, P. (2005) Impact of humans on the flux of terrestrial sediment to the global coastal ocean. *Science* **308**, 376–380.
- Wang, H., Yang, Z., Saito, Y., Liu, J. P. & Sun, X. (2007) Stepwise decreases of the Huanghe (Yellow River) sediment load (1950–2004): impacts from climate changes and human activities. *Global Planetary Change* **57**(3–4), 331–354.